

Synthetic Ion Channel Formed by Multiblock Amphiphile with Anisotropic Dual-Stimuli-Responsiveness

Ryo Sasaki, Kohei Sato,* Kazuhito V. Tabata, Hiroyuki Noji, and Kazushi Kinbara*

Cite This: *J. Am. Chem. Soc.* 2021, 143, 1348–1355

Read Online

ACCESS |

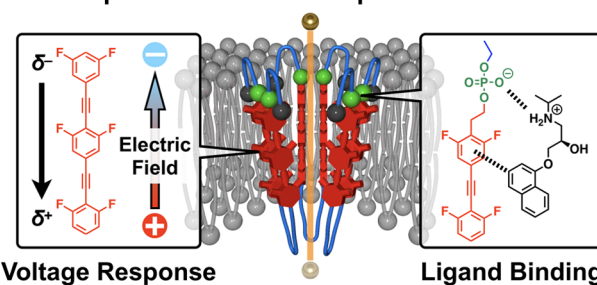
Metrics & More

Article Recommendations

Supporting Information

ABSTRACT: Transmembrane proteins within biological membranes exhibit varieties of important functions that are vital for many cellular activities, and the development of their synthetic mimetics allows for deep understanding in related biological events. Inspired by the structures and functions of natural ion channels that can respond to multiple stimuli in an anisotropic manner, we developed multiblock amphiphile V_F in this study. When V_F was incorporated into the lipid bilayer membranes, V_F formed a supramolecular ion channel whose ion transport property was controllable by the polarity and amplitude of the applied voltage. Microscopic emission spectroscopy revealed that V_F changed its molecular conformation in response to the applied voltage. Furthermore, the ion transport property of V_F could be reversibly switched by the addition of (*R*)-propranolol, an aromatic amine known as an antiarrhythmic agent, followed by the addition of β -cyclodextrin for its removal. The highly regulated orientation of V_F allowed for an anisotropic dual-stimuli-responsiveness for the first time as a synthetic ion channel.

Anisotropic Dual-Stimuli-Responsive Ion Channel



INTRODUCTION

Directional signal transductions across biological membranes are vital for a variety of cellular activities.^{1,2} In many cases, such biological events are carried out by transmembrane proteins within the membranes that respond to various external stimuli such as light, ligand molecules, and changes in pH.^{3–10} Among them, dual-stimuli-responsive transmembrane proteins are particularly intriguing, because they can integrate multiple types of signals and realize their functional controls in a highly precise manner.^{11–14} For example, the transient receptor potential melastatin 8 (TRPM8) channel responds to transmembrane potential and ligand molecules and regulates its directional transmembrane ion transport property to control signal transmissions of neurons.^{15–18} Importantly, the orientation of the TRPM8 channel is highly biased to one side of the membranes so that it can distinguish the difference between intra- and extracellular environments and respond to external stimuli in an anisotropic manner.^{12,19,20} In particular, its charged channel-forming domains respond to the changes in transmembrane potential, which subsequently induce conformational changes of the whole channel.^{21,22} Furthermore, the channel possesses binding pockets for ligand molecules so that it can modulate its ion transport property in response to their bindings.^{23,24}

The goal of this work has been to develop a synthetic molecule that can mimic the functions of such a natural ion channel with anisotropic dual-stimuli-responsiveness. Such an attempt allows for further understandings in related biological events and realizes the development of novel biosensors that

can respond to biologically important signals.^{25,26} Over the past four decades, synthetic molecules that can respond to a single external stimulus such as voltage, ligand molecules, light, or changes in pH have been developed, and their ion transport properties have been investigated.^{27–57} For example, some molecules were designed to possess dipole moments along their molecular axes so that their channel-forming properties could be controlled by the changes in transmembrane potential.^{27–32} Other examples incorporated binding sites for ions and molecules within their structures to control the ion transport properties.^{35–47} However, design and synthesis of such molecules still remain challenging,⁵⁸ and most importantly, no successful example of a synthetic ion channel with anisotropic dual-stimuli-responsiveness has been reported to date.

Meanwhile, in order to develop fully synthetic ion channels that mimic structures and functions of transmembrane proteins in nature, varieties of multiblock amphiphiles have been designed in our group.^{46,47,59,60} It has been demonstrated that these amphiphiles were incorporated into the lipid bilayer membranes vertical to the membrane axis and self-assembled

Received: September 2, 2020

Published: January 14, 2021



to form supramolecular ion channels. Furthermore, their structural flexibility allowed for dynamic regulations of their ion transport properties.^{46,47,60} Based on the molecular designs established in our group and previously reported synthetic channels that can respond to a single external stimulus, dimeric multiblock amphiphile V_F and its monomeric analogue I_F were newly designed (Figure 1a). An asymmetric and a flexible

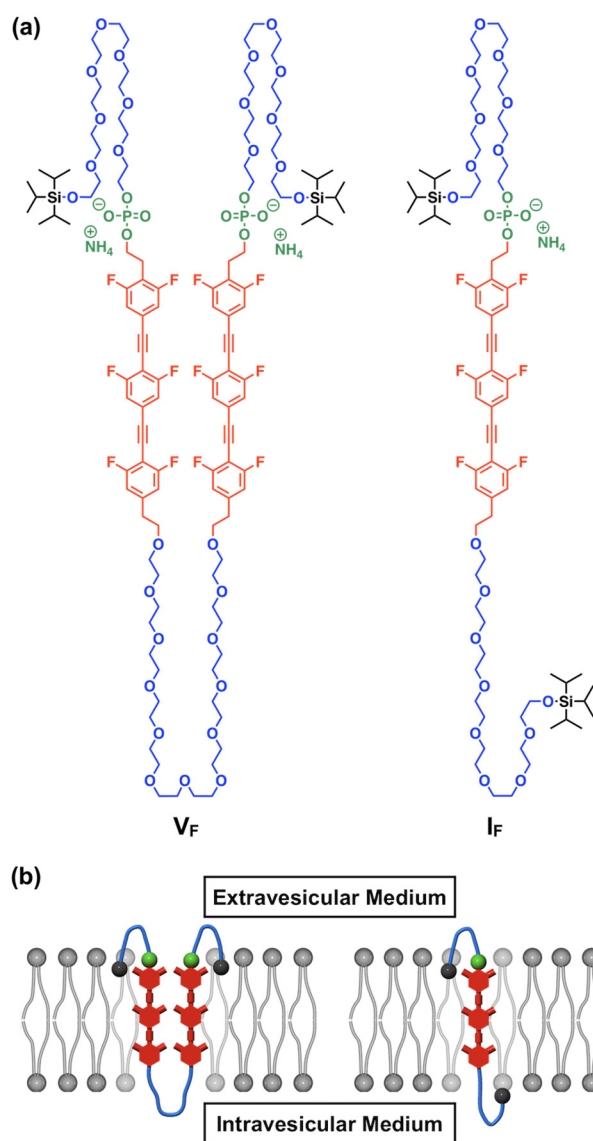


Figure 1. (a) Molecular structures of V_F and I_F . (b) Schematic illustrations of V_F and I_F being incorporated into the lipid bilayer membranes with phosphate ester groups (light green) facing an extravesicular medium. V_F adopts a folded conformation within the membranes.

multipass transmembrane structure of V_F is reminiscent of the structural features of TRP channel family members.⁶¹ We therefore anticipated that the development of such multiblock amphiphiles will give rise to anisotropic dual-stimuli-responsiveness and bring about important progress in this field.

RESULTS AND DISCUSSION

V_F and I_F were designed to incorporate phosphate ester groups, which are important for controlling the molecular orientations across the membranes. Moreover, phosphate ester

groups, which are connected to aromatic units, are expected to interact with ligand molecules such as aromatic amines.⁴⁷ In addition, V_F and I_F consist of oligo(phenylene-ethynylene) moieties as hydrophobic units and oligoethylene glycol (OEG) chains as hydrophilic units (Figure 1a). OEG chains with 8 or 12 repeating units were selected so that these multiblock amphiphiles would effectively span across the lipid bilayer membranes (Figure S85, see Supporting Information).⁴⁷ The hydrophobic unit is functionalized with six fluorine atoms that generate a permanent dipole moment along the molecular axis. Based on DFT calculation, the dipole moment within the hydrophobic unit was evaluated to be 4.4 debyes (Figure S83). The hydrophobic unit of V_F and I_F was synthesized using a Sonogashira cross-coupling reaction, and OEG chains were introduced to the hydrophobic unit by Williamson ether synthesis. An octaethylene glycol chain bearing a phosphate ester group was then coupled by a phosphoramidite method (see Supporting Information). All the newly synthesized compounds were unambiguously characterized by ¹H, ¹³C, ¹⁹F, and ³¹P NMR spectroscopy and high-resolution ESI-TOF mass spectrometry (Figures S1–S82), and the purity of V_F and I_F was further confirmed by elemental analysis (see Supporting Information).

To investigate whether V_F and I_F can be incorporated into the lipid bilayer membranes, microscopic observations of giant unilamellar vesicles (GUVs) that incorporated V_F or I_F were carried out (Figures S86 and S87).^{62,63} GUVs were prepared from 1,2-dioleoyl-*sn*-glycero-3-phosphocholine (DOPC), and V_F or I_F was then added to the dispersion of GUVs. The phase-contrast microscopy visualized the formation of micrometer-sized GUVs (Figures S86a and S87a). Subsequently, fluorescence microscopic observation of the GUVs was performed ($\lambda_{\text{ex}} = 330\text{--}385\text{ nm}$; $\lambda_{\text{obsd}} > 420\text{ nm}$), and emissions along the vesicular edges were clearly observed (Figures S86b and S87b). Because the hydrophobic unit within V_F and I_F is emissive upon excitation by UV light (Figure S88), these results indicate that V_F and I_F were successfully incorporated into the lipid bilayer membranes.

To further study the location of V_F and I_F within the lipid bilayer membranes, fluorescence depth quenching experiments were carried out using spin-labeled phospholipids. Because the quenching of emission depends on the distance between spin probes and target molecules, the location of V_F and I_F can be estimated by varying the position of spin probes within the membranes.⁶⁴ For this purpose, three spin-labeled phospholipids, 1-palmitoyl-2-stearoyl-(*X*-doxyl)-*sn*-glycero-3-phosphocholine ($X = 5:5\text{-doxyl PC}$, $X = 12:12\text{-doxyl PC}$, and $X = 16:16\text{-doxyl PC}$), which bear spin probes at different positions within the alkyl tail, were used. After the preparation of large unilamellar vesicles (LUVs) formed by DOPC and these spin-labeled phospholipids, V_F or I_F was added to the preformed LUVs. As a result, LUVs that incorporated either V_F or I_F showed enhanced degree of quenching for 12- and 16-doxyl PC-containing LUVs in comparison with 5-doxyl PC-containing LUVs (Figure S88). Therefore, the hydrophobic unit within V_F and I_F is not located at the membrane surface but rather in the middle of the lipid bilayers, vertical to the membrane axis (Figure 1b).^{47,59,60,64}

Next, the orientation of V_F and I_F to the membrane axis was investigated to assess whether it would be biased to one side of the lipid bilayer membranes. As mentioned above, such a controlled orientation of ion channels across biological membranes is crucial for their anisotropic dual-stimuli-

responsiveness.^{12,19} Following a previously established method in our group using zeta potential measurements,⁴⁷ approximately 93% of I_F was evaluated to be oriented with its phosphate ester group facing the extravesicular medium (Figures 1b and S89). In addition, 92% of phosphate ester groups within V_F were evaluated to be oriented to the same direction (Figure S90), thus indicating a folded conformation of V_F within the membranes as reported in our previous research (Figure 1b).^{46,47} As mentioned above, V_F or I_F was added to the preformed LUVs. It seems the highly polar phosphate ester groups within the amphiphiles prevented their permeation across the hydrophobic layer of the membranes, and therefore, orientation of V_F and I_F across the lipid bilayer membranes was highly biased.

With the highly regulated orientation of V_F and I_F in hand, their ion transport properties with transmembrane potential were investigated using DOPC black lipid membranes (BLMs) under applied voltages. The BLM was formed horizontally at the orifice and sandwiched with *cis* (upper) and *trans* (lower) chambers (Figure S84, see Supporting Information). First, the BLM without V_F or I_F was confirmed not to allow any ions to permeate across the membranes under the voltage range (-120 to $+120$ mV) tested in this study (Figure S91). Then, V_F or I_F was added from the *cis* (upper) chamber so that V_F and I_F would be oriented with their phosphate ester groups facing the *cis* (upper) chamber (Figure S84). When positive voltage at $+60$ mV was applied, V_F -containing BLM did not show any current flows (Figure 2a). Based on the controlled orientation of V_F , the applied electric field vector under these conditions should be parallel to the dipole moment of V_F . Quite intriguingly, upon application of negative voltage at -60 mV, with an electric field vector antiparallel to the dipole moment of V_F , the current flowed extensively with a maximum value of -2.1 pA (Figure 2b). These results indicate that when the applied electric field vector is antiparallel to the dipole moment of V_F , its transmembrane ion transport property emerges. Then, the average currents over the total recording time under different voltages (\bar{I} - V plot) were plotted (see Supporting Information), and a nonlinear correlation was observed (Figure 2c). This nonlinear profile clearly demonstrated that V_F transports ions in response to the polarity and amplitude of the applied voltage.⁶⁵ As expected, when V_F was introduced from the opposite side of the BLM, the profile showed the similar correlation but with an opposite sign (Figure 2d). It is noteworthy that the observed threshold voltage of ion transport by V_F (ca. 40 mV) is similar to that of voltage-gated potassium channels found in mammalian neurons (30 mV).⁶⁶ Interestingly, the BLM that incorporated I_F showed only slight current flows under positive and negative voltages at even ± 120 mV (Figure S92). The ion transport assay using 8-hydroxypyrene-1,3,6-trisulfonate (HPTS), a pH-sensitive fluorescent dye, also revealed that I_F does not transport ions across the membranes (Figure S93). These results indicate that the dimeric structure of V_F is essential for the voltage-responsive ion transport.

To assess the mechanism of voltage-responsive ion transport by V_F , HPTS assays using variable concentrations of V_F were conducted (Figures S94 and S95). Hill analysis on V_F verified the Hill coefficient of $n = 2.7$ ($R^2 = 0.99$), indicating that V_F self-assembles to form supramolecular ion channels (Figure S94). The molecular diffusion assay using 5-carboxy-fluorescein (5-CF) ensured that the observed ion transport was not due to the nonspecific disruption of the membranes

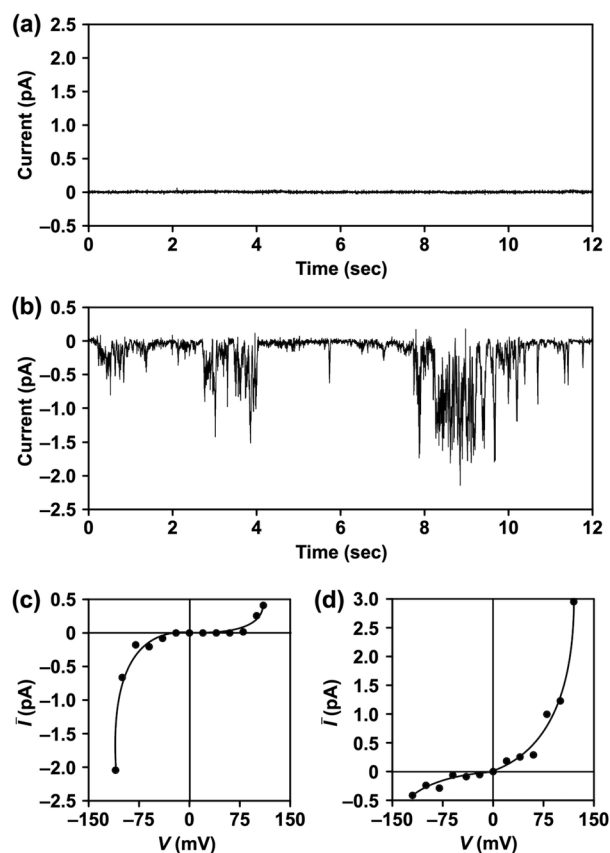


Figure 2. (a,b) Current recordings of V_F -containing BLMs ($[DOPC] = 106 \mu\text{M}$, $[V_F] = 5 \text{ nM}$) in HEPES buffer ($[HEPES] = 20 \text{ mM}$, $[NaCl] = 50 \text{ mM}$, pH 7.5) at the applied voltages of (a) $+60$ mV and (b) -60 mV at 20°C . V_F was added from the *cis* (upper) chamber. (c,d) Plots of average currents over the total recording time (\bar{I}) as a function of applied voltage (V). V_F was added from (c) the *cis* (upper) chamber and (d) the *trans* (lower) chamber, respectively.

caused by supramolecular ion channels formed by V_F (Figure S96).^{67,68} Then, based on the current recording profile of V_F -containing BLM (Figure 2b), a histogram of the current intensity was created, and the most frequent current was observed at -0.49 pA (Figure S97). Using the Hill equation,^{65,69} the pore diameter of the supramolecular ion channel was thus evaluated to be 0.26 nm at the applied voltage of -60 mV (see Supporting Information). Considering the Hill coefficient and the pore diameter, a single supramolecular ion channel is likely formed by the assembly of three molecules of V_F .^{47,51,59,60,70} The observed transient current in Figure 2b also implies the highly dynamic nature of the supramolecular ion channel.²⁸ Then, microscopic emission spectroscopy of BLM that incorporated V_F or I_F was performed under applied voltages (Figure 3a–c). Our previous research demonstrated that such oligo(phenylene-ethynylene) chromophores show red-shifted emissions when they are stacked in a face-to-face manner within the lipid bilayer membranes.^{62,63} Without voltage (0 mV), V_F -containing BLM showed an emission maximum at 441 nm (Figure 3a, blue curve). Then, negative voltages with an electric field vector antiparallel to the dipole moment of V_F were applied, and an abrupt red shift at -40 mV with an emission maximum at 452 nm was observed (Figure 3a,c). In a clear contrast, when positive voltages with an electric field vector parallel to the dipole moment of V_F were applied, the emission maximum did

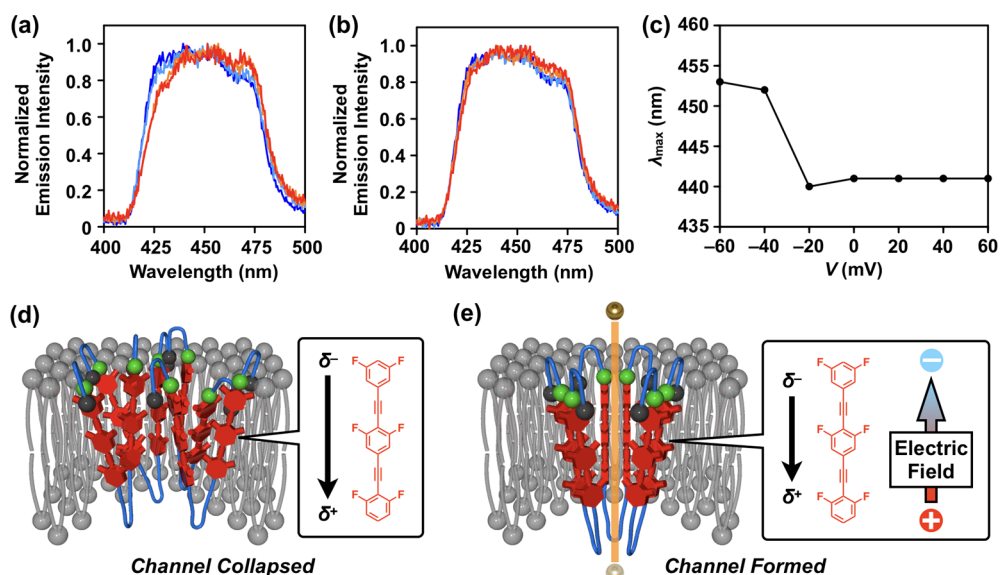


Figure 3. (a,b) Microscopic emission spectra of V_F -containing BLMs ($[DOPC] = 106 \mu\text{M}$, $[V_F] = 1 \mu\text{M}$) in HEPES buffer ($[HEPES] = 20 \text{ mM}$, $[\text{NaCl}] = 50 \text{ mM}$, pH 7.5) at applied (a) negative and (b) positive voltages (0 (blue), ± 20 (pale blue), ± 40 (orange), ± 60 mV (red)) at 20°C ($\lambda_{ex} = 320\text{--}353 \text{ nm}$). V_F was added from the *cis* (upper) chamber. (c) Plot of corresponding emission peak tops as a function of applied voltage. The peak top values were obtained from moving average curves of emission spectra. (d,e) Schematic illustrations of supramolecular ion channels formed by V_F (d) without and (e) with an applied negative voltage. Black arrows represent vectors of dipole moments of V_F .

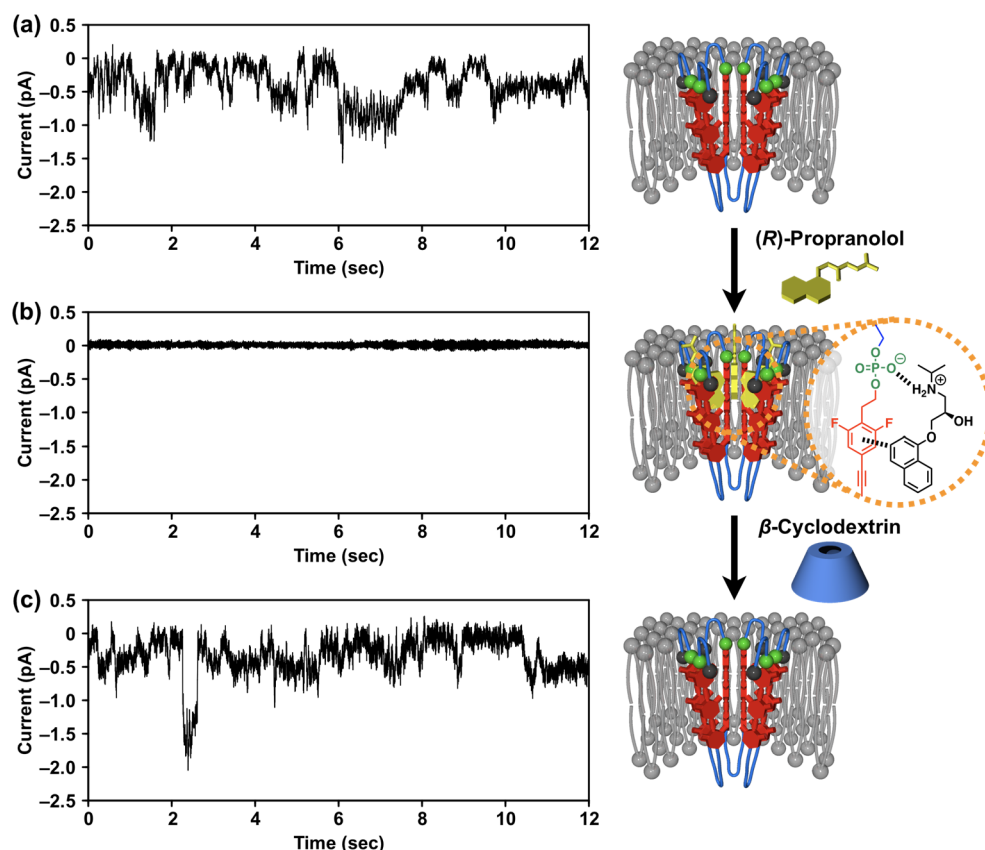


Figure 4. (a–c) Current recordings of V_F -containing BLMs ($[DOPC] = 106 \mu\text{M}$, $[V_F] = 5 \text{ nM}$) in HEPES buffer ($[HEPES] = 20 \text{ mM}$, $[\text{NaCl}] = 50 \text{ mM}$, pH 7.5) at the applied voltage of -60 mV (a) before and (b) after the addition of (*R*)-propranolol ($[(R)\text{-propranolol}] = 200 \text{ nM}$) from the *cis* (upper) chamber, (c) followed by the addition of β -cyclodextrin ($[\beta\text{-cyclodextrin}] = 1 \text{ mM}$) from the *cis* (upper) chamber at 20°C . V_F was added from the *cis* (upper) chamber. Schematic illustrations of the ligand response of V_F are shown on the right side of the corresponding current recordings.

not show any obvious shifts (Figure 3b,c). These spectral changes in response to the change in transmembrane potential

showed a good agreement with the threshold voltage observed in a \bar{I} - V plot (Figure 2c). These results demonstrated that the

stacking manner of the chromophores of V_F and its ion transport property are strongly correlated with the polarity and amplitude of the applied voltage. In particular, when an applied electric field vector is antiparallel to the dipole moment of V_F , face-to-face stacking of its chromophore is enhanced, and the ion transport property emerges. Interestingly, I_F -containing BLMs hardly showed clear changes in emissions under the same voltage range (Figure S98). This result indicates that an intramolecular face-to-face stacking of the chromophores of V_F is crucial for the observed ion transport. Because an intermolecular aromatic interaction is generally known to be weaker than that of an intramolecular aromatic interaction,^{71,72} I_F did not form supramolecular ion channels.

Considering the fact that a flip-flop of phosphate-containing amphiphilic molecules hardly occurs within the lipid bilayer membranes,⁷³ it should be reasonable to hypothesize that the reason for the voltage-responsive ion transport by V_F is mainly due to its electronic polarization rather than its orientation polarization. As mentioned above, V_F adopts a folded conformation within the lipid bilayer membranes, whose dipole moments of two hydrophobic units are positioned in parallel to each other. Therefore, without an application of voltage, hydrophobic units of V_F repel each other so that V_F would not form functional transmembrane ion channels (Figure 3d). However, when a voltage with an electric field vector antiparallel to the permanent dipole moment of V_F is applied, displacement of electron distribution within V_F should occur.⁷⁴ It then creates an induced dipole moment within V_F , whose vector is opposite to the permanent dipole moment of V_F , thereby weakening the net dipole moment of V_F .^{75,76} As a result, the dipole–dipole repulsion between two hydrophobic units of V_F is weakened so that their face-to-face stacking is reinforced, thereby enabling the formation of supramolecular ion channels that can efficiently transport ions across the membranes (Figures 3e). On the other hand, a voltage with an applied electric field vector parallel to the permanent dipole moment of V_F does not weaken the net dipole moment of V_F , and therefore, the ion transport property would not emerge.

Furthermore, the ligand-binding property of V_F was investigated in order to assess the dual-stimuli-responsiveness of the ion channel. For this purpose, (*R*)-propranolol, an antiarrhythmic agent that can block voltage-gated sodium channels, was selected.^{77–80} It is also noteworthy that the use of (*R*)-propranolol is advantageous for current recordings, because it does not deteriorate the membrane stability, while its enantiomer does (Figure S99). ¹H NMR spectroscopy revealed upfield shifts of aromatic and aliphatic protons near the phosphate ester groups of V_F upon the addition of (*R*)-propranolol (Figure S100). These spectral changes indicate that (*R*)-propranolol binds to V_F at its connection part of phosphate esters and hydrophobic units.⁴⁷ In addition, Job's plot revealed that (*R*)-propranolol and V_F form a 1:1 complex, with an association constant of $K_{\text{assoc}} = 9.0 \times 10^3 \text{ M}^{-1}$ ($R^2 = 0.99$) (Figure S101).⁸¹ For current recording measurements, V_F was first added to the DOPC BLM from the *cis* (upper) chamber, so that V_F would be oriented and its phosphate ester groups face the *cis* (upper) chamber (Figure S84). Subsequently, (*R*)-propranolol was added to the V_F -containing BLM from either the *cis* (upper) or *trans* (lower) chamber, and current flows were recorded under negative voltage at -60 mV . As expected, the V_F -containing BLM showed the evident current flows before the addition of (*R*)-propranolol (Figure 4a). Quite intriguingly, after the addition of (*R*)-propranolol to

the BLM from the *cis* (upper) chamber, where the phosphate ester groups of V_F and (*R*)-propranolol are located at the same side of the BLM, a current flow was completely inhibited (Figure 4b). In sharp contrast, when (*R*)-propranolol was added to the BLM from the *trans* (lower) chamber, the current flow was not affected to any significant extent (Figure S102). \bar{I} – V plots under different voltages and HPTS assays further confirmed this trend (Figures S103 and S104). These results clearly demonstrated that the highly regulated orientation of V_F also allowed for an anisotropic response to the ligand molecule. To the best of our knowledge, V_F is the first synthetic ion channel that enabled an anisotropic dual-stimuli-responsiveness. Our previous research demonstrated that (*R*)-propranolol interacts with phosphate ester groups and aromatic units via electrostatic and π – π interactions and localizes inside the channel pore to block the ion transport.⁴⁷ The same mechanism is likely responsible for the observed inhibition of ion transport in this study (Figure 4b).

Finally, with an expectation on the channel reopening, β -cyclodextrin was used as a host molecule for (*R*)-propranolol. Prior to the experiment, the association constant of (*R*)-propranolol and β -cyclodextrin was evaluated to be $K_{\text{assoc}} = 3.3 \times 10^2 \text{ M}^{-1}$ ($R^2 = 0.99$) (Figure S105), based on the 1:1 complexation model reported previously.^{82,83} Then, β -cyclodextrin was added from the *cis* (upper) chamber so that the phosphate ester groups of V_F , (*R*)-propranolol, and β -cyclodextrin would be located at the same side of the BLM. Strikingly, the inhibited current flow was again enhanced to the original level upon the addition of β -cyclodextrin (Figure 4c). Because the BLM with β -cyclodextrin alone does not allow any ions to permeate across the membranes (Figure S106), the observed recovery of the current flow clearly indicates that β -cyclodextrin removed (*R*)-propranolol from the binding site of V_F and reactivated the ion transport property. Such a reversible activation–inactivation cycle is known to be one of the important and ubiquitous features of ion channels in nature, because it prevents the excessive ion flux across the biological membranes to maintain homeostasis.^{84–86}

CONCLUSION

Inspired by natural transmembrane proteins with anisotropic dual-stimuli-responsiveness, we developed a multiblock amphiphile V_F in this study. Ion transport assays using fluorescent dyes in combination with current recordings revealed the formation of supramolecular ion channels by V_F within the lipid bilayer membranes. The permanent dipole moments within the fluorinated hydrophobic units of V_F allowed for controls over its ion transport properties by the polarity and amplitude of the applied voltage. Microscopic emission spectroscopy further revealed that the voltage-triggered conformational change of V_F was responsible for the ion transport. Moreover, the ion transport property of V_F could be inhibited by the addition of (*R*)-propranolol, an antiarrhythmic agent that blocks voltage-gated sodium channels in nature. The highly regulated orientation of V_F allowed for anisotropic responses to the transmembrane potential and a ligand molecule for the first time as a synthetic ion channel. Furthermore, the blocked channel could be reopened by an addition of β -cyclodextrin as a host molecule for (*R*)-propranolol. Because heterogeneous environments across biological membranes are universal features seen in biology, we believe our newly developed synthetic ion channel with anisotropic dual-stimuli-responsiveness possesses a great

potential for sensing and manipulating various biologically important events.

■ ASSOCIATED CONTENT

SI Supporting Information

The Supporting Information is available free of charge at <https://pubs.acs.org/doi/10.1021/jacs.0c09470>.

Details of synthesis, characterization, microscopic studies, spectroscopic studies, zeta potential measurements, current recording studies, and experimental procedures (PDF)

■ AUTHOR INFORMATION

Corresponding Authors

Kazushi Kinbara – School of Life Science and Technology, Tokyo Institute of Technology, Yokohama 226-8501, Japan; orcid.org/0000-0002-5945-9612; Email: kkinbara@bio.titech.ac.jp

Kohei Sato – School of Life Science and Technology, Tokyo Institute of Technology, Yokohama 226-8501, Japan; orcid.org/0000-0002-8948-8537; Email: koheisato@bio.titech.ac.jp

Authors

Ryo Sasaki – School of Life Science and Technology, Tokyo Institute of Technology, Yokohama 226-8501, Japan; orcid.org/0000-0002-5560-881X

Kazuhito V. Tabata – Department of Applied Chemistry, School of Engineering, The University of Tokyo, Tokyo 113-8656, Japan; orcid.org/0000-0002-0463-1374

Hiroyuki Noji – Department of Applied Chemistry, School of Engineering, The University of Tokyo, Tokyo 113-8656, Japan; orcid.org/0000-0002-8842-6836

Complete contact information is available at: <https://pubs.acs.org/10.1021/jacs.0c09470>

Notes

The authors declare no competing financial interest.

■ ACKNOWLEDGMENTS

The authors thank Suzukakedai Materials Analysis Division, Open Facility, Tokyo Institute of Technology, for NMR spectroscopy, EI mass spectrometry, ESI-TOF mass spectrometry, MALDI-TOF mass spectrometry, and elemental analysis. This work was supported by a Grant-in-Aid for Scientific Research on Innovative Areas “Molecular Engine (No. 8006)” (18H05418 and 18H05419 to K.K.), a Grant-in-Aid for Scientific Research B (19H02831 to K.K.), a Grant-in-Aid for Research Activity start-up (18H05971 to K.S.), and a Grant-in-Aid for early-Career Scientists (19H15534 to K.S.). K.S. thanks the Tokyo Institute of Technology for the Yoshinori Ohsumi Fund for Fundamental Research and the ESPEC Foundation for Global Environment Research and Technology (Charitable Trust). We also thank Prof. Hirofumi Shimizu for helpful discussions and Prof. Akira Kato for generous assistance in electrophysiological studies.

■ REFERENCES

(1) Venkatakrishnan, A. J.; Deupi, X.; Lebon, G.; Tate, C. G.; Schertler, G. F.; Babu, M. M. Molecular signatures of G-protein-coupled receptors. *Nature* **2013**, *494*, 185–194.

(2) Shah, R.; Del Vecchio, D. Signaling Architectures that Transmit Unidirectional Information Despite Retroactivity. *Biophys. J.* **2017**, *113*, 728–742.

(3) Luecke, H.; Schobert, B.; Richter, H.-T.; Cartailier, J.-P.; Lanyi, J. K. Structural Changes in Bacteriorhodopsin During Ion Transport at 2 Ångström Resolution. *Science* **1999**, *286*, 255–260.

(4) Govorunova, E. G.; Sineshchekov, O. A.; Janz, R.; Liu, X.; Spudich, J. L. Natural light-gated anion channels: A family of microbial rhodopsins for advanced optogenetics. *Science* **2015**, *349*, 647–650.

(5) Kovalev, K.; Polovinkin, V.; Gushchin, I.; Alekseev, A.; Shevchenko, V.; Borshchevskiy, V.; Astashkin, R.; Balandin, T.; Bratanov, D.; Vaganova, S.; Popov, A.; Chupin, V.; Büldt, G.; Bamberg, E.; Gordeliy, V. Structure and mechanisms of sodium-pumping KR2 rhodopsin. *Sci. Adv.* **2019**, *5*, eaav2671.

(6) Shi, S.-H.; Hayashi, Y.; Petralia, R. S.; Zaman, S. H.; Wenthold, R. J.; Svoboda, K.; Malinow, R. Rapid Spine Delivery and Redistribution of AMPA Receptors After Synaptic NMDA Receptor Activation. *Science* **1999**, *284*, 1811–1816.

(7) Hayashi, Y.; Shi, S.-H.; Esteban, J. A.; Piccini, A.; Poncer, J.-C.; Malinow, R. Driving AMPA Receptors into Synapses by LTP and CaMKII: Requirement for GluR1 and PDZ Domain Interaction. *Science* **2000**, *287*, 2262–2267.

(8) Hansen, S. B.; Tao, X.; MacKinnon, R. Structural basis of PIP₂ activation of the classical inward rectifier K⁺ channel Kir2.2. *Nature* **2011**, *477*, 495–498.

(9) Thompson, A. N.; Posson, D. J.; Parsa, P. V.; Nimigeon, C. M. Molecular mechanism of pH sensing in KcsA potassium channels. *Proc. Natl. Acad. Sci. U. S. A.* **2008**, *105*, 6900–6905.

(10) Jasti, J.; Furukawa, H.; Gonzales, E. B.; Gouaux, E. Structure of acid-sensing ion channel 1 at 1.9 Å resolution and low pH. *Nature* **2007**, *449*, 316–323.

(11) Julius, D.; Basbaum, A. I. Molecular mechanism of nociception. *Nature* **2001**, *413*, 203–210.

(12) Nilius, B.; Owsianik, G. The transient receptor potential family of ion channels. *Genome Biol.* **2011**, *12*, 218.

(13) Dong, Y. Y.; Pike, A. C. W.; Mackenzie, A.; McClenaghan, C.; Aryal, P.; Dong, L.; Quigley, A.; Grieben, M.; Goubin, S.; Mukhopadhyay, S.; Ruda, G. F.; Clausen, M. V.; Cao, L.; Brennan, P. E.; Burgess-Brown, N. A.; Sansom, M. S. P.; Tucker, S. J.; Carpenter, E. P. K₂P channel gating mechanisms revealed by structures of TREK-2 and a complex with Prozac. *Science* **2015**, *347*, 1256–1259.

(14) Lolicato, M.; Arrigoni, C.; Mori, T.; Sekioka, Y.; Bryant, C.; Clark, K. A.; Minor, D. L. K_{2p2.1} (TREK-1)-activator complexes reveal a cryptic selectivity filter binding site. *Nature* **2017**, *547*, 364–368.

(15) Peier, A. M.; Moqrich, A.; Hergarden, A. C.; Reeve, A. J.; Andersson, D. A.; Story, G. M.; Earley, T. J.; Dragoni, I.; McIntyre, P.; Bevan, S.; Patapoutian, A. A TRP Channel that Senses Cold Stimuli and Menthol. *Cell* **2002**, *108*, 705–715.

(16) Voets, T.; Droogmans, G.; Wissenbach, U.; Janssens, A.; Flockerzi, V.; Nilius, B. The principle of temperature-dependent gating in cold- and heat-sensitive TRP channels. *Nature* **2004**, *430*, 748–754.

(17) Nilius, B.; Talavera, K.; Owsianik, G.; Prenen, J.; Droogmans, G.; Voets, T. Gating of TRP channels: a voltage connection? *J. Physiol.* **2005**, *567*, 35–44.

(18) Raddatz, N.; Castillo, J. P.; Gonzalez, C.; Alvarez, O.; Latorre, R. Temperature and Voltage Coupling to Channel Opening in Transient Receptor Potential Melastatin 8 (TRPM8). *J. Biol. Chem.* **2014**, *289*, 35438–35454.

(19) Clapham, D. E. TRP channels as cellular sensors. *Nature* **2003**, *426*, 517–524.

(20) Alberts, B.; Johnson, A.; Lewis, J.; Morgan, D.; Raff, M.; Roberts, K.; Walter, P. Membrane Structure. In *Molecular Biology of the Cell*, 6th ed.; Garland Science: New York, 2014; pp 565–596.

- (21) Voets, T.; Owsianik, G.; Janssens, A.; Talavera, K.; Nilius, B. TRPM8 voltage sensor mutants reveal a mechanism for integrating thermal and chemical stimuli. *Nat. Chem. Biol.* **2007**, *3*, 174–182.
- (22) Fernández, J. A.; Skryma, R.; Bidaux, G.; Magleby, K. L.; Scholfield, N.; McGeown, J. G.; Prevarskaya, N.; Zholos, A. V. Voltage- and cold-dependent gating of single TRPM8 ion channels. *J. Gen. Physiol.* **2011**, *137*, 173–195.
- (23) McKemy, D. D.; Neuhauser, W. M.; Julius, D. Identification of a cold receptor reveals a general role for TRP channels in thermosensation. *Nature* **2002**, *416*, 52–58.
- (24) Yin, Y.; Le, S. C.; Hsu, A. L.; Borgnia, M. J.; Yang, H.; Lee, S.-Y. Structural basis of cooling agent and lipid sensing by the cold-activated TRPM8 channel. *Science* **2019**, *363*, eaav9334.
- (25) Otis, F.; Racine-Berthiaume, C.; Voyer, N. How Far Can a Sodium Ion Travel within a Lipid Bilayer? *J. Am. Chem. Soc.* **2011**, *133*, 6481–6483.
- (26) Hemmatian, Z.; Keene, S.; Josberger, E.; Miyake, T.; Arboleda, C.; Soto-Rodriguez, J.; Baneyx, F.; Rolandi, M. Electronic control of H⁺ current in a bioprotonic device with Gramicidin A and Alamethicin. *Nat. Commun.* **2016**, *7*, 12981.
- (27) Kobuke, Y.; Ueda, K.; Sokabe, M. Totally Synthetic Voltage Dependent Ion Channel. *Chem. Lett.* **1995**, *24*, 435–436.
- (28) Fyles, T. M.; Looock, D.; Zhou, X. A Voltage-Gated Ion Channel Based on a Bis-Macrocyclic Bolaamphiphile. *J. Am. Chem. Soc.* **1998**, *120*, 2997–3003.
- (29) Sakai, N.; Ni, C.; Bezrukov, S. M.; Matile, S. Voltage-dependent Ion Channel Formation by Rigid Rod-shaped Polyols in Planar Lipid Bilayers. *Bioorg. Med. Chem. Lett.* **1998**, *8*, 2743–2746.
- (30) Goto, C.; Yamamura, M.; Satake, A.; Kobuke, Y. Artificial Ion Channels Showing Rectified Current Behavior. *J. Am. Chem. Soc.* **2001**, *123*, 12152–12159.
- (31) Sakai, N.; Houdebert, D.; Matile, S. Voltage-Dependent Formation of Anion Channels by Synthetic Rigid-Rod Push-Pull β -Barrels. *Chem. - Eur. J.* **2003**, *9*, 223–232.
- (32) Wagner, H.; Harms, K.; Koert, U.; Meder, S.; Boheim, G. Oligo-THF Peptides: Synthesis, Membrane Insertion, and Studies of Ion Channel Activity. *Angew. Chem., Int. Ed. Engl.* **1996**, *35*, 2643–2646.
- (33) Si, W.; Li, Z.-T.; Hou, J.-L. Voltage-Driven Reversible Insertion into and Leaving from a Lipid Bilayer: Tuning Transmembrane Transport of Artificial Channels. *Angew. Chem., Int. Ed.* **2014**, *53*, 4578–4581.
- (34) Su, G.; Zhang, M.; Si, W.; Li, Z.-T.; Hou, J.-L. Directional Potassium Transport through a Unimolecular Peptide Channel. *Angew. Chem., Int. Ed.* **2016**, *55*, 14678–14682.
- (35) Fuhrhop, J.-H.; Liman, U.; Koesling, V. A Macrocyclic Tetraether Bolaamphiphile and an Oligoamino α,ω -Dicarboxylate Combine To Form Monolayered, Porous Vesicle Membranes, Which Are Reversibly Sealed by EDTA and Other Bulky Anions. *J. Am. Chem. Soc.* **1988**, *110*, 6840–6845.
- (36) Tedesco, M. M.; Ghebremariam, B.; Sakai, N.; Matile, S. Modeling the Selectivity of Potassium Channels with Synthetic, Ligand-Assembled π Slides. *Angew. Chem., Int. Ed.* **1999**, *38*, 540–543.
- (37) Gorteau, V.; Perret, F.; Bollot, G.; Mareda, J.; Lazar, A. N.; Coleman, A. W.; Tran, D.-H.; Sakai, N.; Matile, S. Synthetic Multifunctional Pores with External and Internal Active Sites for Ligand Gating and Noncompetitive Blockage. *J. Am. Chem. Soc.* **2004**, *126*, 13592–13593.
- (38) Talukdar, P.; Bollot, G.; Mareda, J.; Sakai, N.; Matile, S. Ligand-Gated Synthetic Ion Channels. *Chem. - Eur. J.* **2005**, *11*, 6525–6532.
- (39) Kiwada, T.; Sonomura, K.; Sugiura, Y.; Asami, K.; Futaki, S. Transmission of Extramembrane Conformational Change into Current: Construction of Metal-Gated Ion Channel. *J. Am. Chem. Soc.* **2006**, *128*, 6010–6011.
- (40) Wilson, C. P.; Webb, S. J. Palladium(II)-gated ion channels. *Chem. Commun.* **2008**, *34*, 4007–4009.
- (41) Wilson, C. P.; Boglio, C.; Ma, L.; Cockroft, S. L.; Webb, S. J. Palladium(II)-Mediated Assembly of Biotinylated Ion Channels. *Chem. - Eur. J.* **2011**, *17*, 3465–3473.
- (42) Haynes, C. J. E.; Zhu, J.; Chimere, C.; Hernández-Ainsa, S.; Riddell, I. A.; Ronson, T. K.; Keyser, U. F.; Nitschke, J. R. Blockage Zn₁₀L₁₅ Ion Channels through Subcomponent Self-Assembly. *Angew. Chem., Int. Ed.* **2017**, *56*, 15388–15392.
- (43) Boccalon, M.; Iengo, E.; Tecilla, P. Metal-Organic Transmembrane Nanopores. *J. Am. Chem. Soc.* **2012**, *134*, 20310–20313.
- (44) Talukdar, P.; Bollot, G.; Mareda, J.; Sakai, N.; Matile, S. Synthetic Ion Channels with Rigid-Rod π -Stack Architecture that Open in Response to Charge-Transfer Complex Formation. *J. Am. Chem. Soc.* **2005**, *127*, 6528–6529.
- (45) Peters, A. D.; Borsley, S.; della Sala, F.; Cairns-Gibson, D. F.; Leonidou, M.; Clayden, J.; Whitehead, G. F. S.; Vitorica-Yrezabal, I. J.; Takano, E.; Burthem, J.; Cockroft, S. L.; Webb, S. J. Switchable foldamer ion channels with antibacterial activity. *Chem. Sci.* **2020**, *11*, 7023–7030.
- (46) Muraoka, T.; Endo, T.; Tabata, K. V.; Noji, H.; Nagatoishi, S.; Tsumoto, K.; Li, R.; Kinbara, K. Reversible Ion Transportation Switch by a Ligand-Gated Synthetic Supramolecular Ion Channel. *J. Am. Chem. Soc.* **2014**, *136*, 15584–15595.
- (47) Muraoka, T.; Noguchi, D.; Kasai, R. S.; Sato, K.; Sasaki, R.; Tabata, K. V.; Ekimoto, T.; Ikeguchi, M.; Kamagata, K.; Hoshino, N.; Noji, H.; Akutagawa, T.; Ichimura, K.; Kinbara, K. A synthetic ion channel with anisotropic ligand response. *Nat. Commun.* **2020**, *11*, 2924.
- (48) Stankovic, C. J.; Heinemann, S. H.; Schreiber, S. L. Photo-modulated ion channels based on covalently linked gramicidins. *Biochim. Biophys. Acta, Biomembr.* **1991**, *1061*, 163–170.
- (49) Lien, L.; Jaikaran, D. C. J.; Zhang, Z.; Woolley, G. A. Photomodulated Blocking of Gramicidin Ion Channels. *J. Am. Chem. Soc.* **1996**, *118*, 12222–12223.
- (50) Kobuke, Y.; Ohgoshi, A. Supramolecular ion channel containing *trans*-azobenzene for photocontrol of ionic fluxes. *Colloids Surf., A* **2000**, *169*, 187–197.
- (51) Bhosale, S.; Sisson, A. L.; Talukdar, P.; Fürstenberg, A.; Banerji, N.; Vauthey, E.; Bollot, G.; Mareda, J.; Röger, C.; Würthner, F.; Sakai, N.; Matile, S. Photoproduction of Proton Gradients with π -Stacked Fluorophore Scaffolds in Lipid Bilayers. *Science* **2006**, *313*, 84–86.
- (52) Jog, P. V.; Gin, M. S. A Light-Gated Synthetic Ion Channel. *Org. Lett.* **2008**, *10*, 3693–3696.
- (53) Liu, T.; Bao, C.; Wang, H.; Lin, Y.; Jia, H.; Zhu, L. Light-controlled ion channels formed by amphiphilic small molecules regulate ion conduction *via cis-trans* photoisomerization. *Chem. Commun.* **2013**, *49*, 10311–10313.
- (54) Bao, C.; Ma, M.; Meng, F.; Lin, Q.; Zhu, L. Efficient synthetic supramolecular channels and their light-deactivated ion transport in bilayer lipid membranes. *New J. Chem.* **2015**, *39*, 6297–6302.
- (55) Zhou, Y.; Chen, Y.; Zhu, P.-P.; Si, W.; Hou, J.-L.; Liu, Y. Reversible photo-gated transmembrane channel assembled from an acylhydrazone-containing crown ether triad. *Chem. Commun.* **2017**, *53*, 3681–3684.
- (56) Leevy, W. M.; Gokel, M. R.; Hughes-Strange, G. B.; Schlesinger, P. H.; Gokel, G. W. Structure and medium effects on hydrophilic synthetic ion channel toxicity to the bacterium *E. coli*. *New J. Chem.* **2005**, *29*, 205–209.
- (57) Madhavan, N.; Gin, M. S. Increasing pH Causes Fast Anion- and Cation-Transport Rates through a Synthetic Ion Channel. *ChemBioChem* **2007**, *8*, 1834–1840.
- (58) Zheng, S.-P.; Jiang, J.-J.; Lee, A.; Barboiu, M. A Voltage-Responsive Synthetic Cl⁻-Channel Regulated by pH. *Angew. Chem., Int. Ed.* **2020**, *59*, 18920–18926.
- (59) Muraoka, T.; Shima, T.; Hamada, T.; Morita, M.; Takagi, M.; Tabata, K. V.; Noji, H.; Kinbara, K. Ion Permeation by a Folded Multiblock Amphiphilic Oligomer Achieved by Hierarchical Construction of Self-Assembled Nanopores. *J. Am. Chem. Soc.* **2012**, *134*, 19788–19794.

- (60) Muraoka, T.; Umetsu, K.; Tabata, K. V.; Hamada, T.; Noji, H.; Yamashita, T.; Kinbara, K. Mechano-Sensitive Synthetic Ion Channels. *J. Am. Chem. Soc.* **2017**, *139*, 18016–18023.
- (61) Ihara, M.; Hamamoto, S.; Miyanoiri, Y.; Takeda, M.; Kainosho, M.; Yabe, I.; Uozumi, N.; Yamashita, A. Molecular Bases of Multimodal Regulation of a Fungal Transient Receptor Potential (TRP) Channel. *J. Biol. Chem.* **2013**, *288*, 15303–15317.
- (62) Muraoka, T.; Shima, T.; Hamada, T.; Morita, M.; Takagi, M.; Kinbara, K. Mimicking multipass transmembrane proteins: synthesis, assembly and folding of alternating amphiphilic multiblock molecules in liposomal membranes. *Chem. Commun.* **2011**, *47*, 194–196.
- (63) Sasaki, R.; Sato, K.; Kinbara, K. Aromatic Fluorination of Multiblock Amphiphile Enhances Its Incorporation into Lipid Bilayer Membranes. *ChemistryOpen* **2020**, *9*, 301–303.
- (64) Weiss, L. A.; Sakai, N.; Ghebremariam, B.; Ni, C.; Matile, S. Rigid Rod-Shaped Polyols: Functional Nonpeptide Models for Transmembrane Proton Channels. *J. Am. Chem. Soc.* **1997**, *119*, 12142–12149.
- (65) Hille, B. *Ion Channels of Excitable Membranes*, 3rd ed.; Sinauer Associates: Sunderland, MA, 2001.
- (66) Mitterdorfer, J.; Bean, B. P. Potassium Currents during the Action Potential of Hippocampal CA3 Neurons. *J. Neurosci.* **2002**, *22*, 10106–10115.
- (67) Jones, J. E.; Diemer, V.; Adam, C.; Raftery, J.; Ruscoe, R. E.; Sengel, J. T.; Wallace, M. I.; Bader, A.; Cockroft, S. L.; Clayden, J.; Webb, S. J. Length-Dependent Formation of Transmembrane Pores by 3_{10} -Helical α -Aminoisobutyric Acid Foldamers. *J. Am. Chem. Soc.* **2016**, *138*, 688–695.
- (68) Benz, S.; Macchione, M.; Verolet, Q.; Mareda, J.; Sakai, N.; Matile, S. Anion Transport with Chalcogen Bonds. *J. Am. Chem. Soc.* **2016**, *138*, 9093–9096.
- (69) Marquardt, D.; Heberle, F. A.; Greathouse, D. V.; Koeppe, R. E., II; Standaert, R. F.; Van Oosten, B. J.; Harroun, T. A.; Kinnun, J. J.; Williams, J. A.; Wassall, S. R.; Katsaras, J. Lipid bilayer thickness determines cholesterol's location in model membranes. *Soft Matter* **2016**, *12*, 9417–9428.
- (70) Hennig, A.; Fischer, L.; Guichard, G.; Matile, S. Anion-Macrodipole Interactions: Self-Assembling Oligourea/Amide Macrocycles as Anion Transporters that Respond to Membrane Polarization. *J. Am. Chem. Soc.* **2009**, *131*, 16889–16895.
- (71) Newcomb, L. F.; Gellman, S. H. Aromatic Stacking Interactions in Aqueous Solution: Evidence That neither Classical Hydrophobic Effects nor Dispersion Forces Are Important. *J. Am. Chem. Soc.* **1994**, *116*, 4993–4994.
- (72) Heaton, N. J.; Bello, P.; Herradón, B.; del Campo, A.; Jiménez-Barbero, J. NMR Study of Intramolecular Interactions between Aromatic Groups: Van der Waals, Charge-Transfer, or Quadrupole Interactions? *J. Am. Chem. Soc.* **1998**, *120*, 9632–9645.
- (73) Karp, G. *Cell and Molecular Biology: Concepts and Experiments*, 6th ed.; Wiley-VCH: Weinheim, Germany, 2009.
- (74) Gonano, C. A.; Zich, R. E.; Mussetta, M. Definition for Polarization P and Magnetization M Fully Consistent with Maxwell's Equations. *Prog. Electromagn. Res.* **2015**, *64*, 83–101.
- (75) D'Avino, G.; Muccioli, L.; Zannoni, C.; Beljonne, D.; Soos, Z. G. Electronic Polarization in Organic Crystals: A Comparative Study of Induced Dipoles and Intramolecular Charge Redistribution Schemes. *J. Chem. Theory Comput.* **2014**, *10*, 4959–4971.
- (76) Vemulapalli, G. K.; Kukolich, S. G. Why Does a Stream of Water Deflect in an Electric Field? *J. Chem. Educ.* **1996**, *73*, 887–888.
- (77) Frieden, J. M. D. Propranolol as an antiarrhythmic agent. *Am. Heart J.* **1967**, *74*, 283–285.
- (78) Yang, J.; Wang, E.; Zhou, S.; Yang, Q. Effects of (R)- and (S)-propranolol hydrochloride enantiomers on the resonance Rayleigh scattering spectra with erythrosine B as probe and their analytical applications. *Talanta* **2015**, *134*, 754–760.
- (79) Wang, D. W.; Crotti, L.; Shimizu, W.; Pedrazzini, M.; Cantu, F.; De Filippo, P.; Kishiki, K.; Miyazaki, A.; Ikeda, T.; Schwartz, P. J.; George, A. L., Jr Malignant Perinatal Variant of Long-QT Syndrome Caused by a Profoundly Dysfunctional Cardiac Sodium Channel. *Circ.: Arrhythmia Electrophysiol.* **2008**, *1*, 370–378.
- (80) Wang, D. W.; Mistry, A. M.; Kahlig, K. M.; Kearney, J. A.; Xiang, J.; George, A. L., Jr Propranolol blocks cardiac and neuronal voltage-gated sodium channels. *Front. Pharmacol.* **2010**, *1*, 144.
- (81) Thordarson, P. Determining association constants from titration experiments in supramolecular chemistry. *Chem. Soc. Rev.* **2011**, *40*, 1305–1323.
- (82) Hamai, S. Association of Inclusion Compounds of β -Cyclodextrin in Aqueous Solution. *Bull. Chem. Soc. Jpn.* **1982**, *55*, 2721–2729.
- (83) Barros, T. C.; Stefaniak, K.; Holzwarth, J. F.; Bohne, C. Complexation of Naphthylethanols with β -Cyclodextrin. *J. Phys. Chem. A* **1998**, *102*, 5639–5651.
- (84) Mayer, M. L.; Westbrook, G. L.; Guthrie, P. B. Voltage-dependent block by Mg^{2+} of NMDA responses in spinal cord neurones. *Nature* **1984**, *309*, 261–263.
- (85) Johnson, J. W.; Ascher, P. Voltage-dependent block by intracellular Mg^{2+} of *N*-methyl-D-aspartate-activated channels. *Biophys. J.* **1990**, *57*, 1085–1090.
- (86) Wrighton, D. C.; Baker, E. J.; Chen, P. E.; Wyllie, D. J. A. Mg^{2+} and memantine block of rat recombinant NMDA receptors containing chimeric NR2A/2D subunits expressed in *Xenopus laevis* oocytes. *J. Physiol.* **2008**, *586*, 211–225.